Morning Temporal Variations of Shelter-Level Specific Humidity

M. SEGAL

Department of Physics and Astronomy, University of Kansas, Lawrence, Kansas

G. KALLOS

Department of Applied Physics, University of Athens, Athens, Greece

J. BROWN

Forecast Systems Laboratory, National Oceanic and Atmospheric Administration, Boulder, Colorado

M. MANDEL

Israel Meteorological Service, Bet Dagan, Israel

(Manuscript received 14 December 1990, in final form 28 March 1991)

ABSTRACT

The temporal variation of specific humidity during morning hours was evaluated by analytic and numerical model scaling as well as by observational means. The scaling quantified (i) the gradual increase in the shelter specific humidity as the surface temperature inversion is eroded during the morning hours; (ii) the sharp decrease in the shelter specific humidity when the newly developed boundary layer merges with the previous day's elevated neutral layer. The relation of these patterns to the early-morning thermal stratification and the Bowen ratio was estimated. Observational data supported the general features suggested by the scaling evaluations. The applied significance of the presented specific-humidity patterns is outlined.

1. Introduction

The specific humidity at the meteorological shelter height is an important parameter in various applied considerations. For example, evapotranspiration evaluations, cooling tower efficiency computations, morning visibility estimations, and daily forecasting of convective cloudiness are strongly related to the temporal evolution of daytime specific humidity. Therefore, understanding and scaling the factors determining the daily variations of the specific humidity, mostly during summer days, should be useful for various applications. Apparently no general or detailed research in this area has been carried out. Some relevant specific research is reported in Moses et al. (1967), Wetzel (1973), Mahrt (1976, 1991), Coulman (1978), and Wolfe (1985). This paper focuses on general evaluations, and special attention is given to situations leading to sharp moisture drop (SMD) in the shelter specific humidity in the late morning hours. As evaluated in this paper, SMD may be of importance in several applications. Such situations are likely to occur when the nocturnal surface inversion becomes totally eroded and, consequently, the newly developed atmospheric boundary layer (ABL) is merged with a dry layer of weak thermal stratification above it. In order to evaluate the temporal variations in the specific humidity due to this process, the rates of surface evaporation and breakup of the surface inversion have to be considered.

Scaling and numerical model evaluations of the temporal change in the specific humidity are provided in section 2. Observational examples of sharp temporal changes in the meteorological shelter specific humidity are given in section 3. Various applied aspects associated with the late-morning SMD are evaluated in section 4.

2. Scaling and numerical model evaluations

Morning temporal variations of shelter-level specific humidity are evaluated using scaling and numerical modeling approaches. It is assumed that following sunrise a radiatively induced, surface-based temperature inversion layer of depth h_i exists, and a layer of nearly neutral stratification of appreciable depth Δh is above it, left over from the previous day's ABL. This is commonly observed, for example, in the High Plains of the United States during summer.

Corresponding author address: Moti Segal, Dept. of Physics and Astronomy, University of Kansas, Lawrence, KS 66045-2151.

a. Scaling evaluations

The breakup of the surface inversion layer after sunrise generates a mixing layer. Its depth as a function of time $h(t)$ can be approximated as (e.g., Tennekes 1973)

$$h(t) = \left(\frac{2 \int_0^t H_S dt'}{\rho C_p \beta_0} \right)^{1/2}, \quad (1)$$

where

ρ = the air density
C_p = the specific heat of air at constant pressure
β_0 = the potential temperature lapse rate at sunrise (reflecting an initial thermal stratification)

The daily variation of the surface sensible heat flux H_S and the latent heat flux H_L can be approximated as

$$H_S = H_{So} \sin\left(\frac{\pi t}{D}\right) \quad (2a)$$

$$H_L = H_{Lo} \sin\left(\frac{\pi t}{D}\right), \quad (2b)$$

where H_{So} and H_{Lo} are the noon values of H_S and H_L, respectively, and D is duration of the sunny hours.

Assume for scaling purposes that within the newly developed boundary layer (i.e., as a result of the surface inversion breakup) the specific humidity is well mixed. Its change with time $\eta(t)$, because of surface evapotranspiration during the breakup of the surface inversion process, can be estimated as

$$\eta(t) = \frac{\langle \Delta q \rangle}{\rho h(t)}$$

$$= \frac{(\rho C_p \beta_0)^{1/2}}{\rho L} \frac{\int_o^t [H_{Lo} \sin(\pi t'/D) dt']}{\left[2 \int_0^t H_{So} \sin(\pi t'/D) dt'\right]^{1/2}}$$

$$= \frac{1}{L}\left[\frac{DC_p}{2\pi\rho} \beta_0 \left(1 - \cos\frac{\pi t}{D}\right)\right]^{1/2} \left(\frac{H_{Lo}}{B_0}\right)^{1/2}, \quad (3a)$$

where B_0 is the noon Bowen ratio and L is the latent heat of evaporation. Note that the diurnal variation in the Bowen ratio is ignored in this analysis. In Eq. (3a) $\langle \Delta q \rangle$ is the surface evapotranspiration mass moisture contribution per unit area by time t and it is computed by time integration of Eq. (2b). Assuming for scaling purposes a uniform vertical distribution of the specific humidity at sunrise, Eq. (3a) suggests that, in general, there is a temporal increase in the specific humidity within the newly developed ABL in the morning hours. This increase is larger for more intense stratification in the morning surface temperature inversion (as reflected by β_0) and for smaller B_0. Immediately after the final inversion breakup, the moisture is mixed within a boundary layer of depth $h_i + \Delta h$, resulting in an average increase in the ABL specific humidity η given by

$$\eta \approx \frac{\langle \Delta q \rangle}{\rho(h_i + \Delta h)}. \quad (3b)$$

Note the following.

(i) B_0 is the noon Bowen ratio value when the final breakup of the surface inversion occurs after noon.

(ii) B_0 reduces with increased background temperature level, resulting in reduced ABL development (see, e.g., evaluations in Segal et al. 1989).

(iii) The early-morning lapse rate within the surface-based inversion layer β_0 is commonly observed to decrease slowly with height. Therefore, $\eta(t)$ computed from (3a) using a near-surface value of β_0 is likely to be a slight overestimate.

The dependence of $\eta(t)$ on β_0 and B_0 described by (3a) is depicted by the nomogram in Fig. 1. Summer conditions were assumed, with $H_{Lo} = 500$ W m^{-2} when $B_0 \to 0$. It was also assumed for scaling purposes that H_{Lo} decreases linearly on a log–log scale with increases in B_0, where $B_0 = 15$ when $H_{Lo} \to 0$ (see Segal et al. 1990 for additional details). Periods of $t = 2$ h (Fig. 1a), $t = 4$ h (Fig. 1b), and $t = 6$ h (Fig. 1c) after the commencement of the inversion breakup were chosen. The increase of $\eta(t)$ with the reduction in B_0 is most noticeable for $B_0 < 1$. Also, for $B_0 < 1$ note the increase in $\eta(t)$ with increase in β_0. For high B_0 values, the surface evapotranspiration contribution to the newly developing ABL is small; thus, the variations in $\eta(t)$ for this range of B_0 are quite mild. Similarly, when $\beta_0 \to 0$, the development of the ABL is fast and the values of $\eta(t)$ tend to be low.

It is worth noting that Eq. (3a) indicates that under winter conditions with the same values of B_0 as in summer, the values of $\eta(t)$ will be lower because the winter H_{Lo} is typically lower. Further reduction in the winter $\eta(t)$ values compared to the summer values is likely to be caused by the lower background temperature, which tends to increase the value of B_0. On the other hand, in the winter, β_0 tends to be larger than in summer, offsetting somewhat the above trends. For further elaboration see Segal et al. (1989).

In the general case, early-morning specific humidity varies within the surface inversion layer. Assuming a linear variation with height, change with time of the specific humidity during the inversion breakup process $\eta^*(t)$ can be approximated as

$$\eta^*(t) = \eta(t) + \left[q_0 + 0.5 \frac{dq_0}{dz} h(t)\right], \quad (3c)$$

where q_0 is the early-morning surface specific humidity. Over relatively wet surfaces, however, $\eta(t)$ is likely to be the dominating term in this last expression.

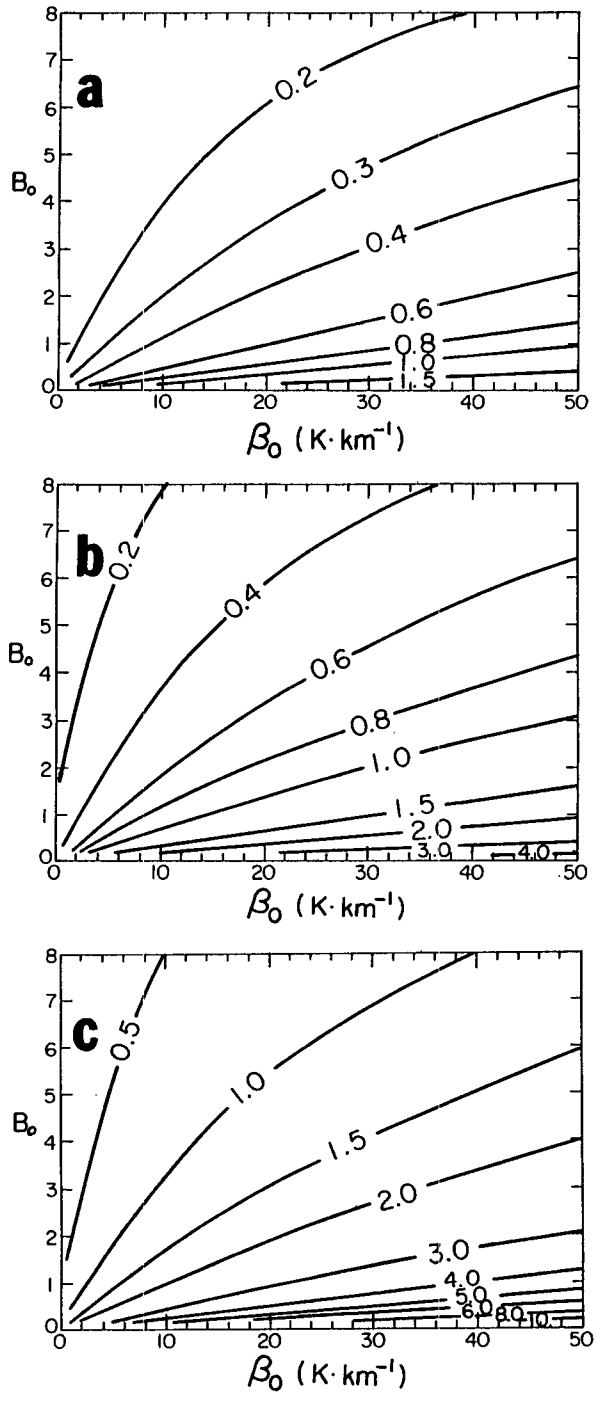

FIG. 1. The dependence of $\eta(t)$ (g kg^{-1}) as derived in Eq. (3) on initial surface potential temperature lapse β_0 and the noon Bowen ratio B_0: (a) 2 h following sunrise, (b) 4 h following sunrise, and (c) 6 h following sunrise.

b. *Numerical model simulations*

One-dimensional numerical model simulations were carried out to complement the scaling given in section 2a. As in the previous scaling evaluations, horizontal advection of moisture is not considered. In real-world situations, however, advection may occasionally play an important role in establishing the moisture stratification during the morning hours. The formulation of the numerical model adapted for these evaluations is given in Mahrer and Pielke (1977) and McNider and Pielke (1981) and, therefore, is not repeated here. The model was reasonably validated against observations by Segal and Mahrer (1979), McNider and Pielke (1981), and Segal and Pielke (1981), among others. The input parameters and initial conditions for the model simulations are given in Table 1.

Two sets of numerical model simulations were carried out. In case C1, the surface moisture availability m was varied between 0.05 and 0.4 for a given thermal stratification (β_0 = 20 K km^{-1} for $z \leq 300$ m; β_0 = 0 K km^{-1} for $300 < z \leq 4000$ m; above 4000 m, a standard atmosphere lapse rate was used). The surface moisture availability equals the ratio of the surface evaporation to the potential evaporation. As such, it provides an indication of the surface moisture level. A value of m = 0.05 indicates a relatively dry surface, whereas m = 0.4 indicates a relatively wet surface. In case C2, a fixed value of m = 0.2 was adopted, where β_0 within the surface stable layer ($z \leq 300$ m) was varied between 5 and 40 K km^{-1}, and was kept as in case C1 for $z > 300$ m.

In case C1, the breakup of the surface inversion is delayed with increasing values of m (Fig. 2a). For $m \leq 0.1$, the final breakup of the surface inversion and onset of deep convective ABL occurred between 1100 and 1200 LST, whereas for the very wet surface (m = 0.4), this stage was simulated only around 1400 LST.

TABLE 1. Model basic input parameters and initial conditions.

Parameter		Value
Surface roughness		0.04 m
Soil specific heat		1330 J kg^{-1} K^{-1}
Soil density		1500 kg m^{-3}
Soil diffusivity	for $m \leq 0.2$	3.10^{-7} m^2 s^{-1}
	for $m > 0.2$	6.10^{-7} m^2 s^{-1}
Surface albedo		0.2
Model levels (m) = 1, 3, 10, 25, 50, 75, 100, 125, 150, 175, 200, 225, 250, 275, 300, 325, 350, 375, 400, 450, 500, 600, 700, 800, 900, 1000, 1250, 1500, 1750, 2000, 2500, 3000, 3500, 4000, 4500, 5000, 6000, 7000, and 9000.		
Initial specific-humidity profile (g kg^{-1}) at the model levels (0500 MST July 1977–80 average for Denver): = 6.7, 6.6, 6.6, 6.6, 6.6, 6.5, 6.3, 6.1, 6.0, 5.9, 5.8, 5.7, 5.6, 5.5, 5.4, 5.3, 5.2, 5.1, 4.9, 4.9, 4.9, 4.8, 4.8, 4.8, 4.8, 4.8, 4.6, 4.5, 4.3, 3.9, 3.6, 3.6, 3.2, 2.7, 2.2, 1.4, 0.4, 0.4, and 0.4.		
Initial potential temperature		as specified in the text
Synoptic flow		5 m s^{-1}
Beginning of the simulation		0600 LST
Day of the year		15 July
Latitude		40°N

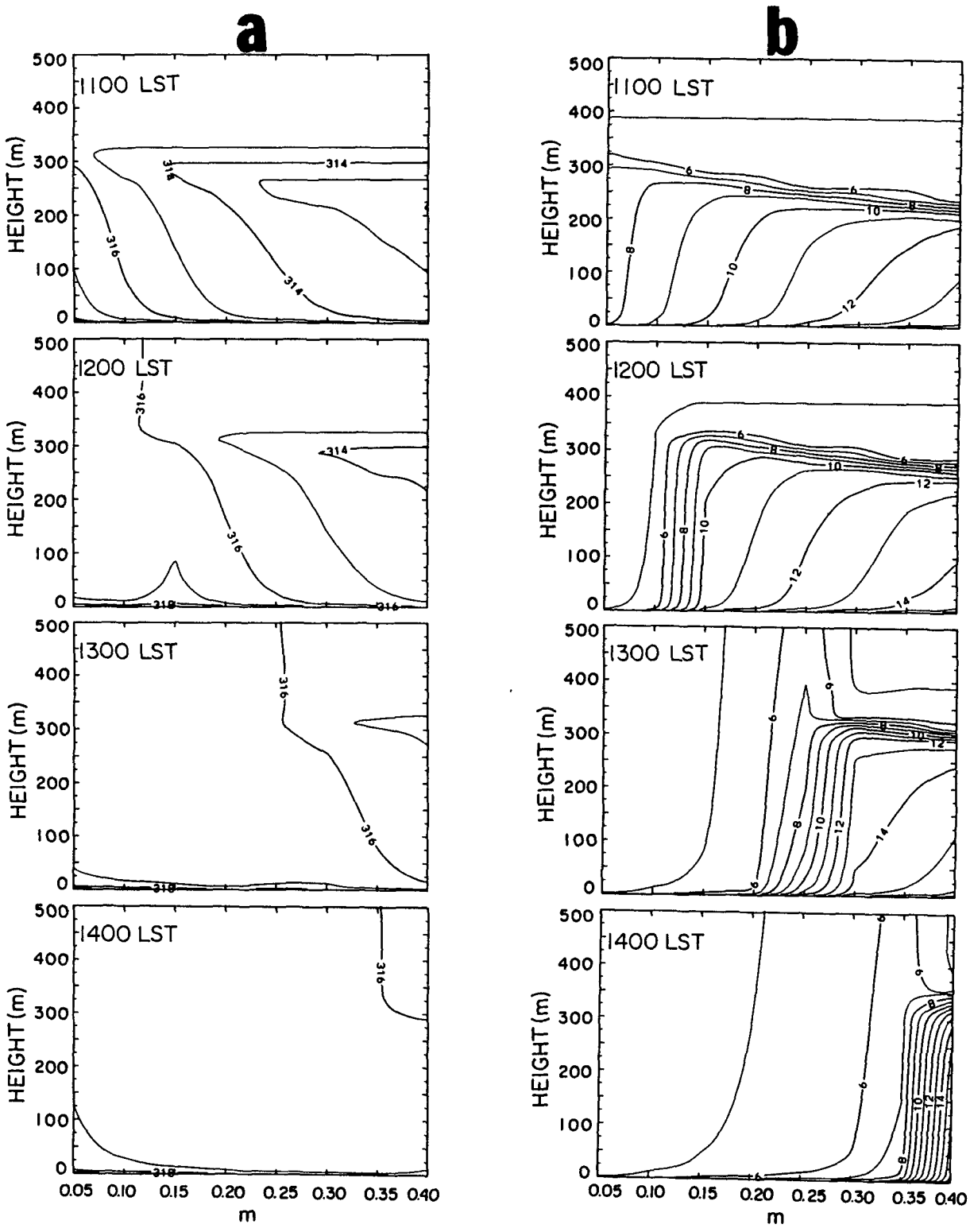

FIG 2. Results of simulations with case C1. (a) Potential temperature (K) and (b) specific humidity (g kg^{-1}) are depicted as a function of height and surface moisture availability m for the stated hours.

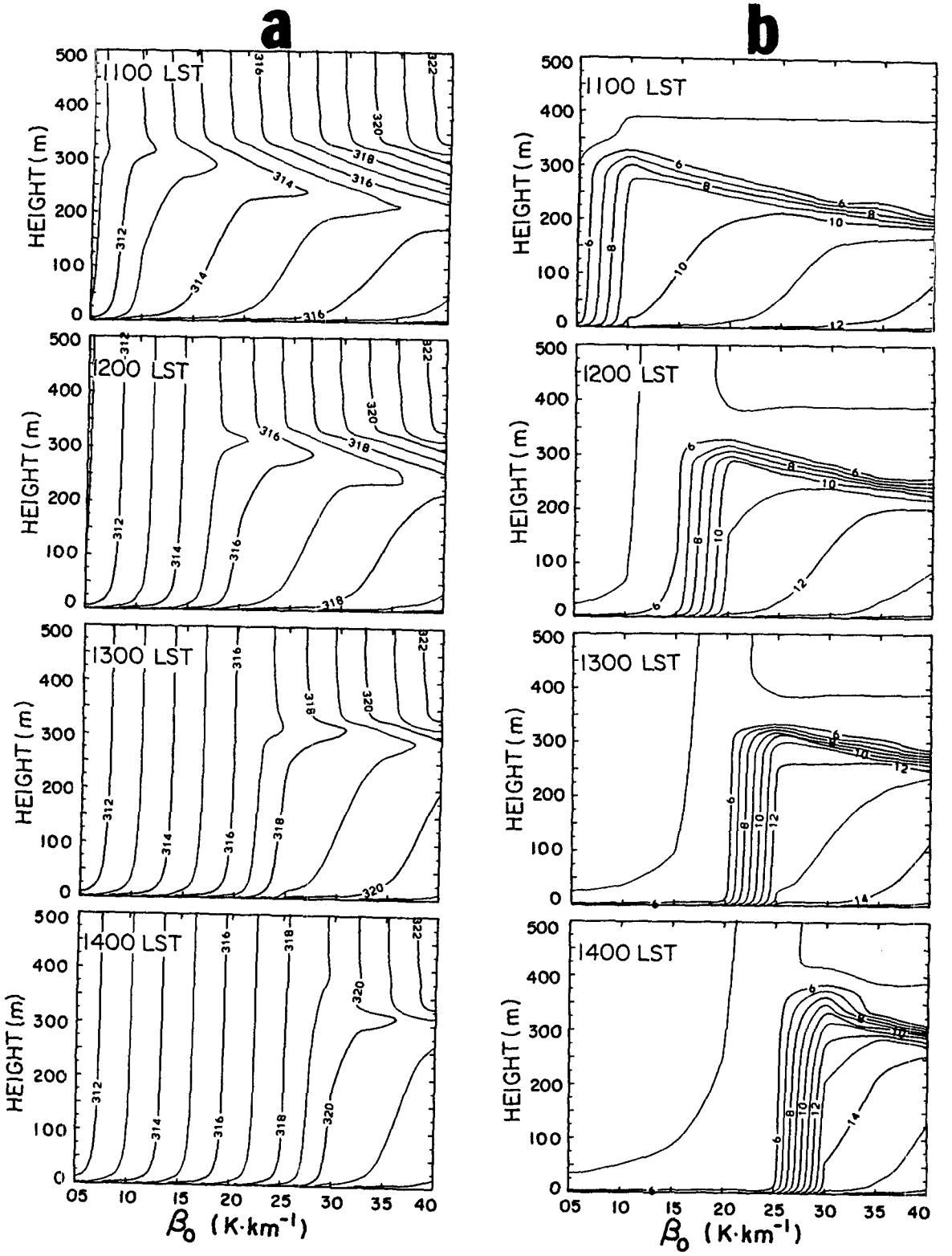

FIG. 3. Results of simulations with case C2. (a) Potential temperature (K) and (b) specific humidity (g kg^{-1}) are depicted as function of height and β_0 for the stated hours.

The accumulation of moisture within the newly developed ABL before the final breakup of the surface inversion (Fig. 2b) increases with the increase in m because of larger evaporation rate and slower breakup of the surface inversion. With the final breakup of the surface inversion and the merging of the newly developed ABL with the deep neutral layer aloft, a sharp decrease in the specific humidity is computed, as implied by Eq. (3b).

In case C2, as anticipated, larger β_0 delays the final breakup of the surface inversion (Fig. 3a). Consequently, similar features described previously for the specific-humidity accumulation are simulated, as is the eventual sharp drop in its level (Fig. 3b). Moisture accumulation within newly developing ABL in the morning hours, followed later by a moisture drop, was observed by Wetzel (1973), Coulman (1978), and Wolfe (1985).

In many applications, as is discussed in section 4, evaluations are made in terms of the shelter dewpoint temperature T_d and the wet-bulb temperature T_w. Therefore, it is useful to present the impacts described in cases C1 and C2 in terms of the temporal variations of T_w and T_d. Figure 4 presents the patterns of the shelter level T_d in cases C1 and C2. Before the final breakup of the surface temperature inversion, increase in T_d is evident. The drop in T_d at the final breakup of the inversion is larger than 6°C and increases somewhat with the increase in m, reaching $\approx$10°C for m = 0.4. As can be inferred from observations of T_d for the Front Range of Colorado, which are presented in section 3, $m \approx 0.2$ is typical for this region. Similar features are computed for case C2 (Fig. 4b). The corresponding variations of T_w for cases C1 and C2 are presented in Fig. 5, where generally similar characteristics to those presented in Fig. 4 were computed.

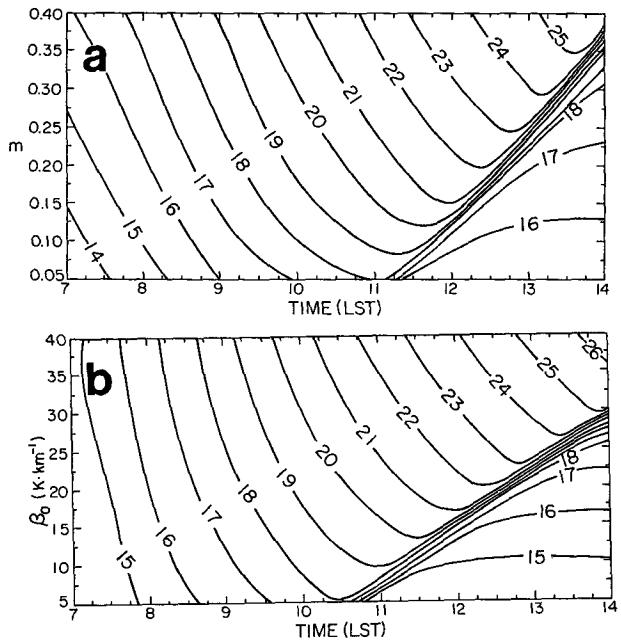

FIG. 5. As in Fig. 4, except for T_w.

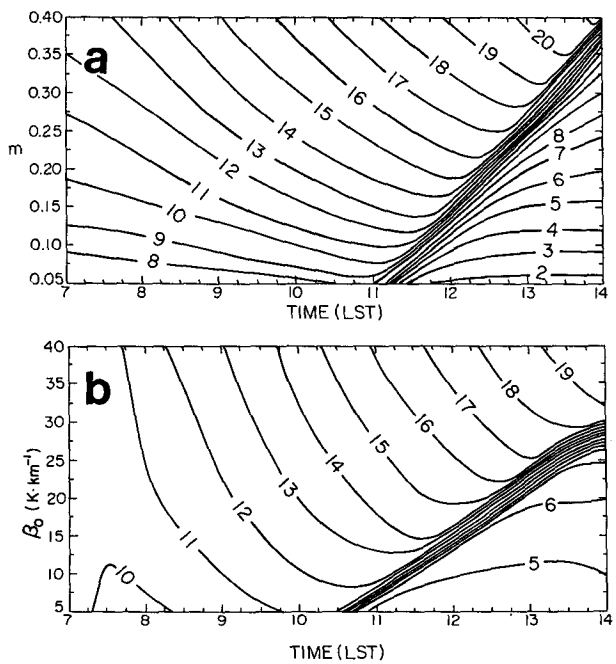

FIG. 4. Temporal variation of the shelter-level dewpoint temperature T_d (°C) as a function of (a) m, case C1, (b) β_0, case C2.

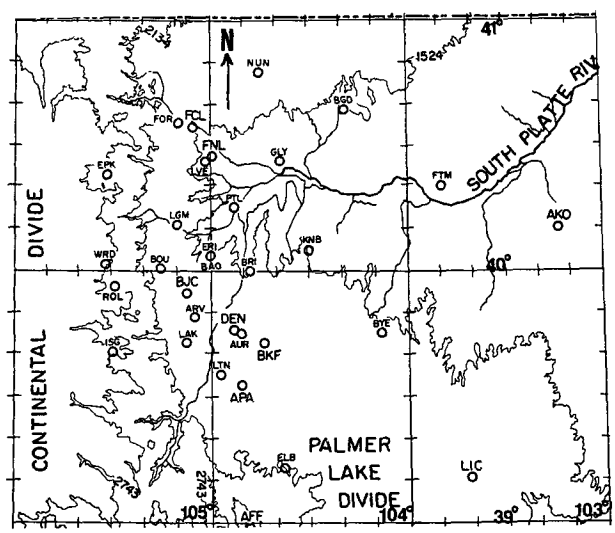

FIG. 6. Illustration of the site locations of the PROFS mesonet stations considered in the study. Also indicated are locations where hourly Standard Airways Observations are made. Relevant to this study are the following sites: AUR–Aurora, BOU–Boulder, DEN–Denver, ERI–Erie, FOR–Fort Collins, GLY–Greeley, LAK–Lakewood, NUN–Nunn. Terrain elevation contours (MSL) are given in intervals of 600 m.

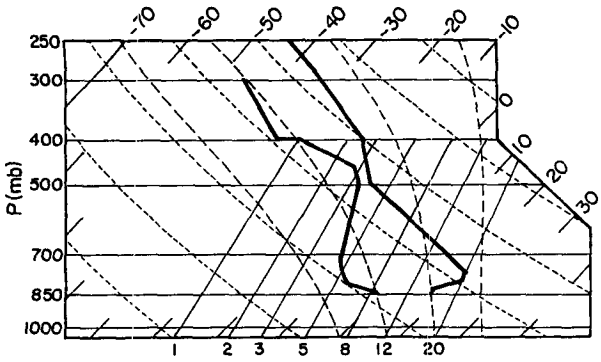

FIG. 7. The Denver skew-T diagram for 0500 MST 11 July 1989; temperature and dewpoint temperature are indicated.

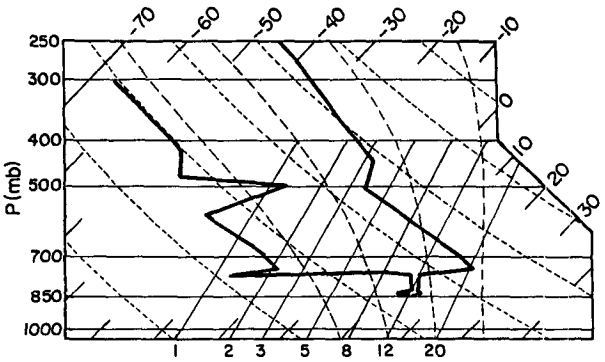

FIG. 9. As in Fig. 7, except for 17 July 1989.

3. Observations

We used the PROFS network to provide observational illustration of the SMD in support of the scaling and modeling evaluations given in section 2. Four cases are described in which the temporal variation of T_d at selected stations is related to the Denver morning thermal and moisture stratification.

The most likely areas to show the late-morning SMD are in geographical locations with relatively deep daytime ABL and with wet surfaces (e.g., crop areas, wet surface because of precipitation events, and to a lesser degree, because of dew). The High Plains of the United States is an example of such a geographical location.

An excellent region for an observational evaluation is the Front Range of Colorado. A deep daytime convective ABL is typical, and nocturnal surface inversions with depths of several hundred meters are common. The area is largely cultivated; thus, surface evapotranspiration can be appreciable. Detailed data for this region are available through NOAA's Forecast Systems Laboratory, formerly the Program for Regional Observing and Forecasting Services (PROFS) (see Reynolds 1983). A network of automated surface observation stations (the location of stations relevant to this study is indicated in Fig. 6) provides 5-min-average measurements (using cooled-mirror hygrometers) of dewpoint temperature.

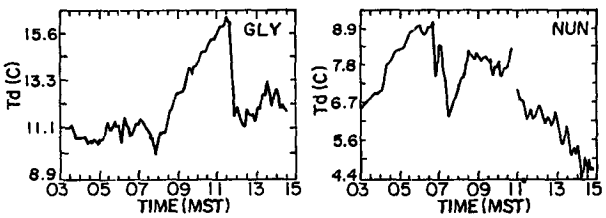

FIG. 8. 11 July 1989, variations of T_d at GLY and NUN.

a. *The 11 July 1989 case*

On 11 July 1989 the Denver 0500 MST (around sunrise) radiosonde indicated a surface temperature inversion with a depth of $\approx$500 m and with intensity of 5°C. Above the inversion layer a near-neutral thermal stratification was observed (Fig. 7). Figure 8 presents the temporal variations of T_d at two illustrative sites. At GLY, the observed pattern of temporal change in T_d is as suggested by the analytical and numerical simulations: gradual increase in T_d during the morning hours followed by a sharp decrease in T_d as the final breakup stage of the surface inversion occurred. At NUN, which is located on relatively higher terrain, the surface inversion is likely to be shallower and less intense. Also, at NUN the surface is somewhat drier than in the cultivated South Platte River basin (in which GLY is located). Therefore, a sustained dewpoint rise does not occur here after sunrise, and the dewpoint drop occurs earlier and is more gradual than at GLY.

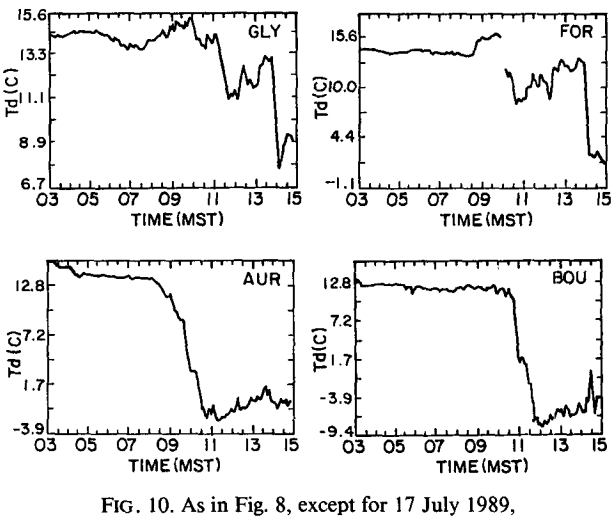

FIG. 10. As in Fig. 8, except for 17 July 1989, and at GLY, FOR, AUR, and BOU.

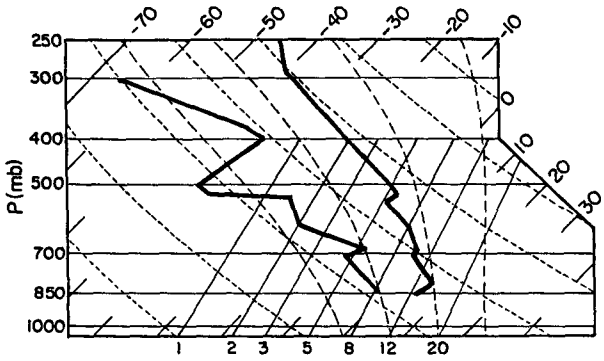

FIG. 11. As in Fig. 7, except for 19 July 1989.

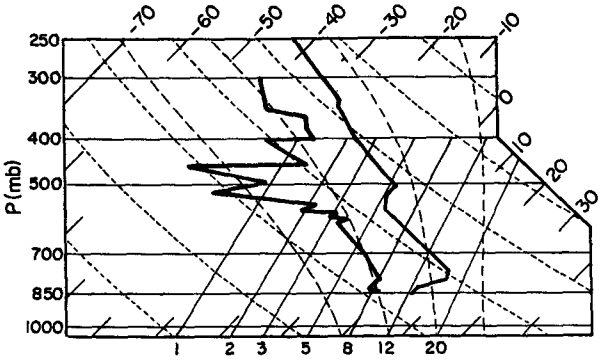

FIG. 13. As in Fig. 7, except for 26 July 1989.

b. *The 17 July 1989 case*

At 0500 MST 17 July 1989 a moist air mass, originating as a precipitation-driven downdraft in convection the previous evening, was observed over the High Plains of northern Colorado. The depth of the nearly pseudoadiabatic moist layer, shown by the Denver radiosonde (Fig. 9), was about 800 m. It was capped by a shallow ($\approx$150 m), intense temperature inversion, followed by a very deep dry layer of near-neutral stratification. This is an uncommon ABL characteristic in the area for the given hour and month; however, it provides an opportunity to examine the temporal changes in the moisture (Fig. 10) under a different thermal structure from that assumed in section 2. Reduction of the early-morning solar radiation at the surface by fog and low stratus and the highly moist lower atmosphere apparently reduced the evapotranspiration rates, causing little or no increase in T_d during the morning hours. At GLY and FOR, the sharp drop in T_d occurred after noon, whereas at AUR and BOU it occurred earlier.

c. *The 19 July 1989 case*

On 19 July 1989 a shallow surface temperature inversion was indicated by the Denver radiosonde, followed aloft by a somewhat stable thermal stratification (Fig. 11). The development of the daytime ABL in the absence of a neutral layer aloft resulted in a more gradual decrease in T_d at GLY and NUN (Fig. 12).

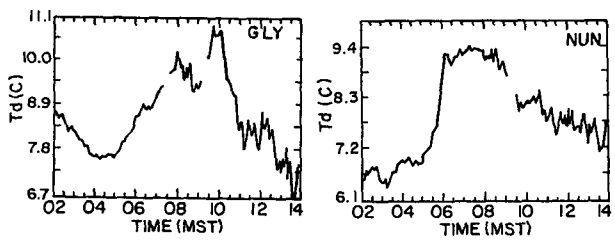

FIG. 12. As in Fig. 8, except for 19 July 1989, and at GLY and NUN.

d. *The 26 July 1989 case*

The 26 July 1989 case involved a surface inversion at Denver in the lower 600 m, followed by a nearly neutral thermal stratification with moderately dry conditions (Fig. 13). The accumulation of moisture in the early hours was not pronounced in all presented sites (Fig. 14). However, the drop in T_d was quite sharp at some of the sites (AUR, ARV).

The presented observational features indicate general agreement with the characteristics suggested by the analytical and numerical evaluations provided in section 2. In three of the presented cases, the moisture at Denver dropped with height within the nocturnal inversion layer. Nevertheless, the morning moisture increase was noticeable. The diurnal changes documented are typically observed at many of the PROFS stations on synoptically quiescent days during the summer. However,

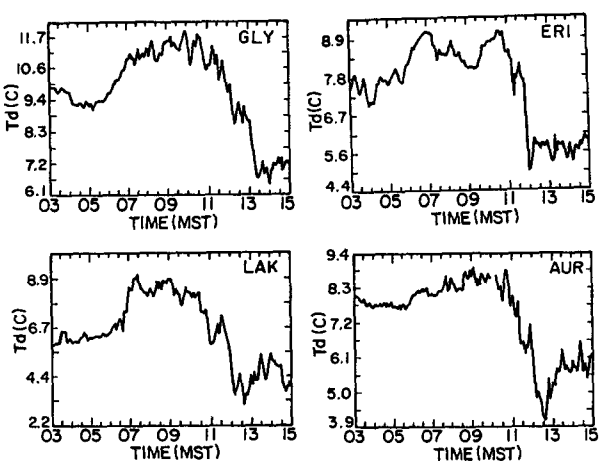

FIG. 14. As in Fig. 8, except for 26 July 1989 and at GLY, ERI, LAK, and AUR.

mountain–valley circulations produced by the high terrain to the west (Johnson and Toth 1985) undoubtedly modulate the idealized trends shown by the simulations of section 2. Further, the Denver sounding may not always be representative of other locations.

4. Some considerations of applied aspects

Temporal variations of moisture at shelter height are important in a variety of applications. Knowledge of the diurnal aspects of moisture climatology and principles useful for moisture prediction may, therefore, be of economical and practical interest. Using the general characteristics of the temporal variation derived from scaling and modeling results as well as the observational examples, we make several conceptual evaluations, focusing on the period of SMD in the near-surface air.

a. Agricultural aspects

Two agricultural aspects are evaluated: the impact of SMD on water losses through sprinkler irrigation, and the increase in evapotranspiration from fields under cultivation because of the increase in air-moisture deficit.

1) SPRINKLER IRRIGATION LOSSES

Sprinkler irrigation water losses are largely related to droplet evaporation and, as such, are related to the air specific-humidity deficit. In ideal dense sprinkler irrigation, the air temperature, which is affected by droplet evaporation, should decrease to the wet-bulb temperature (e.g., Seginer 1973; Kohl and Wright 1974). In the following, the *relative* increase in such water losses as a result of SMD is evaluated.

Based on the definition of the air wet-bulb temperature, the following approximations are applicable for potential water losses δq:

$$\delta q^B = q_s{}^B(T_w) - q_s{}^B(T_d) = (T - T_w{}^B)\frac{C_p}{L} \qquad (4a)$$

$$\delta q^A = q_s{}^A(T_w) - q_s{}^A(T_d) = (T - T_w{}^A)\frac{C_p}{L}, \qquad (4b)$$

where the superscripts B and A indicate relations applicable before and after the SMD. The air temperature T is assumed to be unchanged during the SMD. (Note that the SMD period coincides with the stage of the final eroding of the surface inversion. Therefore, the diurnal increase in the shelter temperature is typically slow during this period.) Using Eqs. (4a) and (4b), the relative increase in the potential evaporative water losses R_L, because of SMD is given by

$$R_L = \frac{\delta q^A}{\delta q^B} = \left(1 + \frac{\Delta T_w}{\Delta T^B}\right), \qquad (5)$$

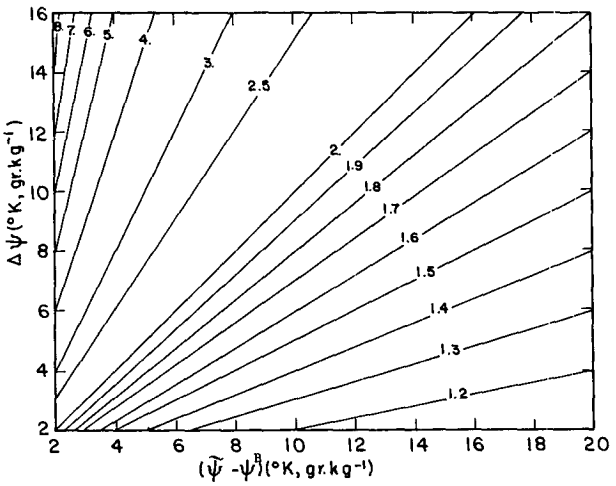

FIG. 15. Nomogram representing the value of $1 + \Delta\psi(\tilde{\psi} - \psi^B)^{-1}$, where $\psi = T_w$(K) and $\tilde{\psi} = T$(K) when using Eq. (5); $\psi = q_a$(g kg^{-1}) and $\tilde{\psi} = q_s$ when used for evaluations associated with Eqs. (6)–(10). See notation definition in section 4.

where $\Delta T_w = T_w{}^B - T_w{}^A$ and $\Delta T^B = T - T_w{}^B$. The nomogram presented in Fig. 15 provides the values of R_L for various possible combinations of ΔT_w and ΔT^B. For example, when $\Delta T_w = \Delta T^B$, the amount of water lost by evaporation is doubled.

Forecasting of the daily SMD period and its intensity may be useful in scheduling daytime irrigation when it is flexible. If possible, daytime irrigation should be stopped after a noticeable SMD.

2) EVAPOTRANSPIRATION LOSSES

For general insight purposes, the increase in evapotranspiration due to SMD is examined, both using the combination equation approach and based on the surface-layer formulation.

(i) *The combination equation approach*

We evaluate the SMD effect using two expressions: theoretical relation and empirical formula. Using the so-called combination formulation (Penmann 1956; Monteith 1981), we can theoretically approximate the evaporation rate for a highly wet surface as

$$H_L = \frac{1}{L}\frac{s}{s+\gamma}(R_N - G^*) + \frac{\gamma\rho}{s+\gamma}\frac{\delta q_a}{r_a}, \qquad (6)$$

where

R_N = the net radiation at the surface,
G^* = the soil thermal flux at the surface or equivalent flux in a case of canopy-covered surface,
$s = dq_s/dT$, with q_s the saturated specific humidity at temperature T,
$\gamma = C_p/L$, which is the psychrometric constant,

$\delta q_a = q_s - q_a$, the specific-humidity deficit at the reference level in the air,

r_a = the bulk aerodynamic resistance to water vapor transfer (assumed the same as for heat transfer; $r_a \approx 100$ s m^{-1}) between the surface and reference level z.

In Eq. (6), the first term of the right-hand side is the energy term and the second term represents the aerodynamical effects. In a first approximation the change in H_L during SMD is expressed by the second term.

An alternative simplified approximation for Eq. (6), though for the potential evapotranspiration, is given by the Priestley–Taylor (1972) empirical equation:

$$E_p = \frac{\alpha}{L}\left(\frac{s}{s+\gamma}\right)(R_N - G^*), \tag{7}$$

where α is constant. Using Eq. (6), we show that

$$\alpha = 1 + \left(\frac{\gamma}{s}\right)\frac{\rho L \delta q_a}{(R_N - G^*)r_a}. \tag{8}$$

From the observational data of Priestley and Taylor, $\alpha \approx 1.26$. The impact of the SMD on E_p is reflected by increase in α.

The relative increase in the aerodynamic term in Eq. (6) as result of the SMD is given by $1 + \Delta q_a(q_s - q_a{}^B)^{-1}$, where Δq_a is the drop in the air specific humidity caused during the SMD, and $q_a{}^B$ is the air specific humidity before the SMD. The relative increase in $1 - \alpha$ is also given by that expression. The nomogram given in Fig. 15 can also be used to quantify the magnitude of change in these variables.

(ii) *Surface-layer formulation*

We use the surface-layer similarity formulation

$$H_L = \rho L u_* q_*, \tag{9}$$

where u_* is the surface friction velocity and q_* is a surface-layer moisture-difference scalar [$q_* \propto (q_a - q_s)$ with q_s the surface saturation specific humidity].

From Eq. (9), and assuming that q_s is unchanged during the SMD,

$$\frac{H_L{}^A}{H_L{}^B} = \frac{q_a{}^A - q_s}{q_a{}^B - q_s} = 1 + \frac{\Delta q_a}{q_s - q_a{}^B}. \tag{10}$$

The nomogram in Fig. 15 provides a quantitative illustration of Eq. (10). It can be shown that the change in the surface evaporation following SMD estimated with the empirical relations given in Eqs. (6)–(8) and given by Eq. (10) are nearly the same.

b. Effects related to wet-bulb temperature

The wet-bulb temperature T_w is an important parameter in evaluating outdoor comfort indices. Various indices quantifying outdoor comfort use T_w as one of the input parameters (e.g., Thom 1959). Segal and Mahrer (1979) and Segal and Pielke (1981) adopted commonly used temperature–humidity indices that consider the dry- and wet-bulb temperatures. The various ranges of comfort using T_w-related indices are provided in these papers and cited literature therein. A drop of T_d by 5 K (as illustrated in some of the observations presented in section 3) should result in a noticeable change in the comfort indices through their T_w dependence.

Efficiency of cooling-tower performance is related to T_w (and hot and cold water temperatures). According to ASHRE (1988, chapter 20.13, Fig. 22), a drop of several kelvins in T_w will increase very noticeably the efficiency of cooling-tower performance.

c. Air pollution conditions

It is well known that the morning surface radiative temperature inversion is associated with a relatively high pollutant concentration caused by surface emissions. Increased air specific humidity leads to enhanced photochemical reactions. In addition, because of vapor absorption, the increased specific humidity results in increase in aerosol size and, consequently, contributes to deterioration of visibility.

In the morning hours, the increase in air humidity and pollutant concentration within the ABL in many cases is due mostly to surface contributions. Thus, the impact on the level of both following the SMD is likely to be similar. Because of this similarity (note also that pollutant and moisture dispersion characteristics are the same), it is suggested that temporal variations in the specific humidity (or T_d) during the morning hours should provide an indication of the concentration of pollutants emitted on the surface. The reduction in T_d should be accompanied by a decrease in surface-pollutant concentration as well as an improvement in visibility.

d. Forecasting of convection

Reasoning from the scaling arguments and numerical model results of section 2, one may make a qualitative prediction of convective cloudiness later in the day from an early-morning sounding. Indeed, severe-storm forecasters use these general concepts together with careful monitoring of the shelter T and T_d to infer evolution of the thermal and moisture stratification in the lower atmosphere during the day (McGinley 1986).

An effective strategy for predicting convective cloudiness is to use the 1200 UTC radiosonde data to make an early-morning estimate of the likely course of temperature and specific humidity during the day, incorporating the principles discussed here. Then, surface conditions should be monitored closely, watching for significant departures from anticipated trends. Such

departures can be used to infer changes to the initially assumed local thermal and moisture stratification, including changes caused by advection or vertical motion, and then to modify the earlier forecast. Within this context the present study suggests the following.

(i) An SMD of the type evaluated in the present study is a practical indicator of the final eroding of the thermally stable layer in the lower atmosphere and generation of a deep ABL. As such, it is also an indicator of the potential for subsequent convective cloud development. McGinley (1986) therefore suggests usage of SMD in nowcasting of convective clouds. Furthermore, he suggests using improvement of visibility as an indicator that an SMD has occurred (see section 4c). Within this context it is worth pointing out the case study by Fuelberg et al. (1991) in the Cooperative Huntsville Meteorological Experiment. They found a significant SMD over a small portion of central Tennessee that occurred prior to the onset of convective activity along the edges of that location.

(ii) For nowcasting purposes the shelter T_d values prior to the SMD in wet surface areas may give a false indication of the potential for convective-cloud development. Appropriate adjustment considering the near-surface accumulated moisture, as evaluated in the present study, is required.

(iii) The surface evapotranspiration over wet surfaces may be an important source of moisture supply for the ABL. It has to be included in consideration of the local forecast of convective-cloud predictions. During the summer, the daily amount of evapotranspiration may reach 8 mm over such surfaces. Utilizing Eq. (3b) with $h + \Delta h_i = 2000$ m suggests that if the SMD occurs around noon, an average moisture increase of 2 g kg^{-1} in the ABL would be attributable to the surface evapotranspiration.

5. Discussion

The temporal variations of near-surface specific humidity were evaluated by scaling, numerical model simulations, and observations. The significance of these patterns, as related to several applied topics, was outlined and scaled. The summer-morning change of specific humidity in relatively dry areas and over evaporative surfaces is typically associated with a continuous increase and then noticeable drop in near-ground air moisture when the morning surface inversion is entirely eroded. When the surface inversion is capped by a deep neutral stratification, the drop in the specific humidity is sharp and rapid ($\leqslant$1800 s). When the layer above the surface inversion layer is stable, the drop in the specific humidity is likely to be more gradual, because the development of the convective boundary layer is slower.

The temporal variations in surface moisture discussed are quite common during the summer over the High Plains of northern Colorado, as had been established through daily examinations during summer 1989 (results not provided). However, deviation from these features because of mesoscale or synoptic perturbations is not uncommon. Knowing the typical summer temporal variation of the dewpoint temperature, a deviation from it may imply that a specific lower-atmosphere process is underway (e.g., horizontal advection of moisture). Also, the moisture variation pattern may be modified when the background moisture within the inversion layer decreases significantly with height. In this situation, specific humidity increases during the morning hours are not guaranteed.

The present study has not addressed the likelihood of SMD in more humid geographical locations than northeastern Colorado (e.g., the Midwest and the Southeast of the United States). It is suggested that in such regions the daytime ABL depths are lower than those in the High Plains of the United States, and the layer above the nocturnal surface inversion is more humid (and often has higher static stability). Thus, the likelihood of a pronounced SMD effect appears to be reduced in these regions (e.g., Moses et al. 1967).

We have discussed the significance of the SMD phenomenon for various applied considerations. A climatological evaluation of the time of day and frequency of occurrence of the SMD would provide a useful supplement to this study. Daily forecasting of the properties of the ABL, including the time of occurrence of the SMD, would be operationally useful for a number of applications. The model used to construct Figs. 2 and 3 (or a similar model) is suitable for running on a PC.

Acknowledgments. The study was partially supported by NSF Grant ATM86-16662. Computations were carried out at the NCAR Computer Center. Observational data were obtained by the PROFS-SERS at the Cooperative Institute for Research of the Atmosphere (CIRA) at Colorado State University. We would like to thank W. Bausch, H. Duke, S. Harold, T. McKee, J. Purdom, E. Szoke, and J. Weaver for their comments, C. Thomas for editing, and R. Solwa for preparing the manuscript.

REFERENCES

ASHRAE Handbook, 1988: *Equipment.* American Society of Heating, Refrigerating and Air Conditioning Engineers, Inc.

Coulman, C. E., 1978: Boundary-layer evolution and nocturnal inversion dispersal. Part I: *Bound.-Layer. Meteor.*, **14,** 471–491.

Fuelberg, H. E., R. L. Schudalla, and A. R. Guillory, 1991: Analysis of sudden mesoscale drying at the surface. *Mon. Wea. Rev.*, **119,** 1391–1406.

Johnson, R. H., and J. J. Toth, 1985: Summer surface flow characteristics over northeast Colorado. *Mon. Wea. Rev.*, **113,** 1458–1469.

Kohl, R. A., and J. L. Wright, 1974: Air temperature and vapor pressure changes caused by sprinkler irrigation. *Agron. J.*, **66,** 85–88.

Mahrer, Y., and R. A. Pielke, 1977: A numerical study of air flow over irregular terrain. *Contrib. Atmos. Phys.*, **50,** 98–113.

Mahrt, L., 1976: Mixed layer moisture structure. *Mon. Wea. Rev.*, **104,** 1403–1407.

——, 1991: Boundary layer moisture. *Quart. J. Roy. Meteor. Soc.*, **117,** 151–176.

McGinley, J., 1986: Nowcasting mesoscale phenomena. *Mesoscale Meteorology and Forecasting,* P. S. Ray, Ed., Amer. Meteor. Soc., 657–688.

McNider, R. T., and R. A. Pielke, 1981: Diurnal boundary-layer development over sloping terrain. *J. Atmos. Sci.*, **38,** 2198–2212.

Monteith, J. L., 1981: Evaporation and surface temperature. *Quart. J. Roy. Meteor. Soc.*, **107,** 1–27.

Moses, H., W. C. Ashby, and M. Bogner, 1967: Dewpoint temperature inversions. *J. Appl. Meteor.*, **7,** 206–216.

Penmann, H. L., 1956: Evaporation: An introductory survey. *Neth. J. Agric. Sci.*, **4,** 9–29.

Priestley, C. H. B., and R. J. Taylor, 1972: On the assessment of surface heat flux and evaporation using large-scale parameters. *Mon. Wea. Rev.*, **100,** 81–92.

Reynolds, D. W., 1983: Prototype workstation for mesoscale forecasting. *Bull. Amer. Meteor. Soc.*, **64,** 264–273.

Segal, M., and Y. Mahrer, 1979: Heat load conditions in Israel—a numerical mesoscale model study. *Int. J. Biometeor.*, **23,** 270–284.

——, and R. A. Pielke, 1981: Numerical model simulation of biometeorological heat load conditions—summer day case study in the Chesapeake Bay area. *J. Appl. Meteor.*, **20,** 735–749.

——, J. R. Garratt, G. Kallos, and R. A. Pielke, 1989: On the impact of wet soil and canopy temperatures on daytime ABL growth. *J. Atmos. Sci.*, **46,** 3673–3684.

——, X. Jia, Z. Ye, and R. A. Pielke, 1990: On the effect of daytime surface evaporation on pollution dispersion. *Atmos. Environ.*, **24A,** 1801–1811.

Seginer, I., 1973: A note on sprinkler spray evaporation. *Agric. Meteor.*, **11,** 307–311.

Tennekes, H., 1973: A Model for dynamics of inversion above a convective boundary layer. *J. Atmos. Sci.*, **30,** 558–567.

Thom, E. C., 1959: The discomfort index. *Weatherwise,* **12,** 57–60.

Wetzel, P. J., 1973: Moisture surfaces and flow patterns during the northeast Colorado hail season. M. S. thesis, Dept. of Atmospheric Science, Colorado State University, Fort Collins, 90 pp.

Wolfe, D. E., 1985: Early morning evaluation of the convective boundary layer at the Boulder Atmospheric Observatory. M. S. thesis, Dept. of Atmospheric Science, Colorado State University, Fort Collins, 160 pp.